

# Prospects of heavy dark $Z_D$ at multi-TeV muon colliders

Prasenjit Sanyal

CQUeST, Sogang University

Based on Phys.Rev.D 112 (2025) 9, 095010

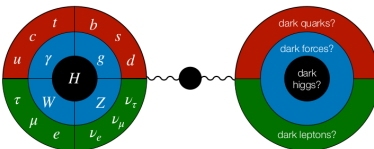
“Probing a Heavy Dark  $Z$  Boson at Multi-TeV Muon Colliders: Leveraging the Optimized Recoil Mass Technique”

Kingman Cheung, Jinheung Kim, Soojin Lee, **Prasenjit Sanyal**, Jeonghyeon Song

1. Why a new dark  $U(1)$  gauge boson? – Commonly referred to as a dark photon  $A'$  or dark gauge boson  $Z_D$ .
2. Existing constraints and projected sensitivities from future experiments in the  $Z_D$  parameter space.
3. Motivations for muon colliders (MuC) as future collider experiment.
4. Search for heavy (TeV scale)  $Z_D$  at MuC via annihilation channel  $\mu^+\mu^- \rightarrow Z_D\gamma$ .

# Why a new dark $U(1)_D$ gauge boson $Z_D$ ?

- Dark matter (DM) particles may interact with each other through a new dark force that is similar to the electromagnetic force felt by ordinary matter.



A schematic representation of the dark-sector paradigm

- The dark gauge boson  $Z_D$  that mediates this force can obtain a small coupling to the electromagnetic current due to kinetic mixing between the SM hypercharge and  $U(1)_D$  field strength tensors via the operator

$$\mathcal{L} \supset \frac{\varepsilon}{2 \cos \theta_W} F'_{\mu\nu} B^{\mu\nu}, \quad \varepsilon \text{ is the kinetic mixing parameter}$$

- The dark  $Z_D$  obtains a mass  $m_{Z_D}$  via a dark Higgs or Stueckelberg mechanism. The minimal dark  $Z_D$  model has only three unknown parameters:  $m_{Z_D}$ ,  $\varepsilon$  and  $Z_D$  to DM branching ratio (1 if kinematically allowed, 0 if forbidden).

(A) DM ( $\chi$ ) is heavier than  $Z_D$  (secluded DM): The DM *freeze-out* is obtained by annihilations to pairs of on-shell  $Z_D$  ( $\chi\chi \rightarrow Z_D Z_D$ ) followed by  $Z_D$  decay to SM particles.

- In this scenario the decay of  $Z_D$  is restricted to the visible (SM) sector only.

(B) DM ( $\chi$ ) is lighter than  $Z_D$ : The DM annihilation is via  $\chi\chi \rightarrow Z_D^* \rightarrow f\bar{f}$

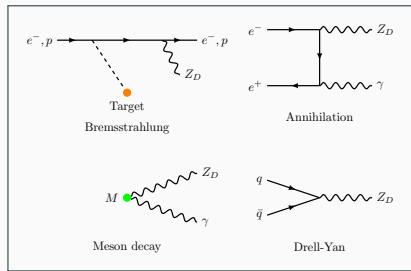
$$\langle\sigma v\rangle \propto \frac{\varepsilon^2 \alpha_D m_\chi^2}{m_{Z_D}^4} \equiv \frac{y}{m_\chi^2}$$

provides thermal target – large  $\varepsilon$  and small  $m_{Z_D}$ .

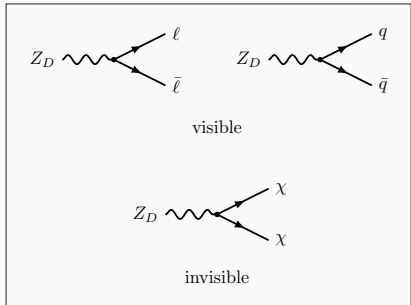
- In this scenario, for  $m_{Z_D} > 2m_\chi$ ,  $Z_D \rightarrow \chi\chi$  decay is nearly 100%.

# Production of $Z_D$ in accelerators

1. Bremsstrahlung:  $e^- Z \rightarrow e^- ZZ_D$  and  $pZ \rightarrow pZZ_D$  where an incident electron or proton radiates  $Z_D$  during an interaction with a fixed nuclear target of charge  $Z$ .
2. Annihilation:  $e^+e^- \rightarrow Z_D\gamma$  at an  $e^+e^-$  collider.
3. Drell-Yan:  $q\bar{q} \rightarrow Z_D$ , where a quark and antiquark annihilate into a  $Z_D$ , which could occur at a hadron collider or when a proton beam is incident on a fixed nuclear target.
4. Meson decays:  $\pi_0 \rightarrow Z_D\gamma$  or  $\eta \rightarrow Z_D\gamma$  for  $m_{Z_D} < m_{\pi_0, \eta}$  at any experiment where mesons are produced at high rates.



**Production of  $Z_D$ :** Bremsstrahlung, Annihilation, Drell-Yan and Meson decay.



Visible (SM fermions) and invisible (DM) decay modes of  $Z_D$ .

## Visible decay:

1. The visible decay modes can be prompt if  $\varepsilon \gtrsim 10^{-3} \times 10\text{MeV}/m_{Z_D}$ .
2. Non-prompt or displaced decay for smaller  $\varepsilon$  and  $m_{Z_D}$ .  $\tau_{Z_D} \propto (\varepsilon^2 m_{Z_D})^{-1}$ .

## Invisible decay:

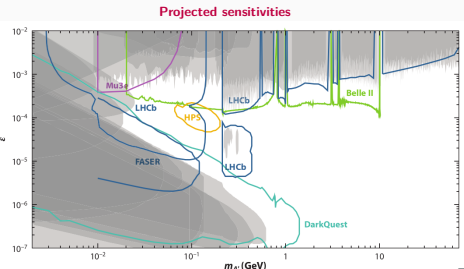
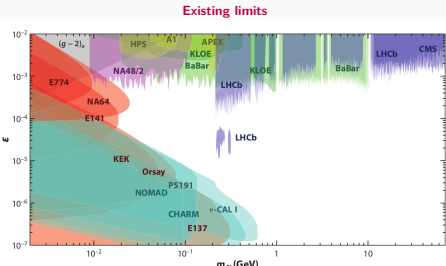
1. if  $m_{Z_D} > 2m_\chi$ ,  $Z_D$  decays to DM by 100%
2. Search strategies look for events with an imbalance of energy and momentum.
3. Search for the rare interactions of the DM particles in a detector placed downstream of the  $Z_D$  decay point.

# Current Constraints and projected sensitivities

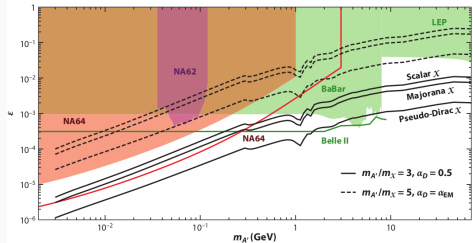
## Visibly decaying $Z_D$ :

1. Current constraints from electron beam dumps (red), proton beam dumps (light blue),  $e^+e^-$  colliders (green),  $pp$  collisions (dark blue), meson decays (purple), and electron-on-fixed-target experiments (yellow).
2. Proposed future sensitivities with the same color schemes.

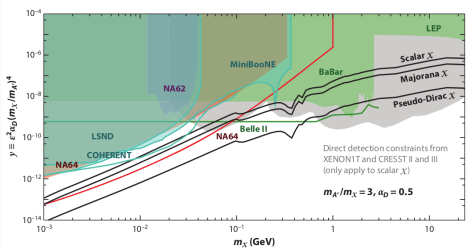
"Searches for dark photons at accelerators", arXiv: 2104.10280



### Existing limits and Projected sensitivities



### Existing limits and Projected sensitivities



### Invisibly decaying $Z_D$ :

1. Constraints and proposed sensitivity from  $e^+e^-$  colliders (green), electron beam dump (red) and meson decay (purple).
2. Constraints on the invisible  $Z_D \rightarrow \chi\chi$  scenario in the  $(m_\chi, y)$  plane. Searches for dark  $Z_D$  produced in proton beam dumps with the subsequent scattering of  $\chi$  particles in a detector placed downstream of the  $Z_D$  decay point are shown using light blue.

"Searches for dark photons at accelerators", arXiv: 2104.10280

# Why Muon Colliders (MuC)?

## Advantages:

1. Future muon colliders (MuC) could be ideal for achieving both high energy and high luminosity.
2. Reduced synchrotron radiation  $\frac{1}{R} \left(\frac{E}{m}\right)^4$ , compared to  $e^+ e^-$  colliders.
3. A few TeV MuC is as efficient as a 100 TeV hadron collider.
4. Much lower background compared to hadron colliders.

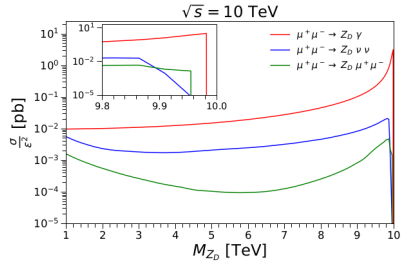
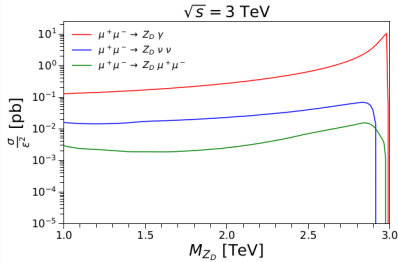
## Disadvantages:

1. Muons are unstable with a lifetime of  $2\mu s$ .
2. Difficult to produce low emittance muon beams.
3. Beam induced backgrounds or BIBs.

**MuC is at the conceptual stage...**

- For a heavy  $Z_D$  with a mass above 1 TeV, constraints become weaker.
- Existing studies have focused on  $pp$  colliders via the Drell-Yan process  $pp \rightarrow Z_D \rightarrow \ell\ell$ .
- At **HL-LHC** (14 TeV &  $3 \text{ ab}^{-1}$ ), the projected sensitivity reaches  $\varepsilon \sim 10^{-2}$  and  $10^{-1}$  for  $m_{Z_D} \sim 1 \text{ TeV}$  and  $2.5 \text{ TeV}$  respectively.
- At **FCC-hh** (100 TeV &  $3 \text{ ab}^{-1}$ ), can improve to  $\varepsilon \sim 4 \times 10^{-3}$  and  $3 \times 10^{-2}$  for  $m_{Z_D} \sim 1 \text{ TeV}$  and  $2.5 \text{ TeV}$  respectively.
- At MuC  $2 \rightarrow 2$  and  $2 \rightarrow 3$  annihilation channels:
  1.  $\mu^+ \mu^- \rightarrow Z_D \gamma$
  2.  $\mu^+ \mu^- \rightarrow Z_D \nu \nu$
  3.  $\mu^+ \mu^- \rightarrow Z_D \mu^+ \mu^-$with  $p_T^{\gamma, \mu} > 10 \text{ GeV}$ ,  $|\eta| < 2.5$  and  $E_{miss}^T > 10 \text{ GeV}$ .

**The  $2 \rightarrow 2$  annihilation  $\mu^+ \mu^- \rightarrow Z_D \gamma$  appears most promising**



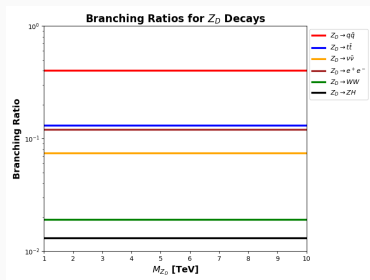
Kingman Cheung, Jinheung Kim, Soojin Lee, **Prasenjit Sanyal**, Jeonghyeon Song,  
 Phys.Rev.D 112 (2025) 9, 095010

## $Z_D$ decay modes

- Two key decay modes at the MuC:  $Z_D \rightarrow jjX$  (inclusive dijet) and  $Z_D \rightarrow e^+e^-$ .
- The inclusive dijet mode combines multiple hadronic final states ( $q\bar{q}$ ,  $t\bar{t}$ ,  $\tau\bar{\tau}$ , and  $WW$ ) maximizes the signal yield.
- $e^+e^-$  mode provides a cleaner final state compared to the  $\mu^+\mu^-$  decay mode.

- The signal is categorized into:

1.  $\mu^+\mu^- \rightarrow Z_D\gamma$ ,  $Z_D \rightarrow jjX$
2.  $\mu^+\mu^- \rightarrow Z_D\gamma$ ,  $Z_D \rightarrow e^+e^-$



## Photon recoil mass

- For the process

$$\mu^+(p_1) + \mu^-(p_2) \rightarrow Z_D(p_{Z_D}) + \gamma(p_\gamma)$$

The recoil mass of the photon is defined as

$$\begin{aligned} m_{\text{recoil}}^2 &= (p_1 + p_2 - p_\gamma)^2 \equiv m_{Z_D}^2 \\ &= s - 2\sqrt{s}E_\gamma \end{aligned}$$

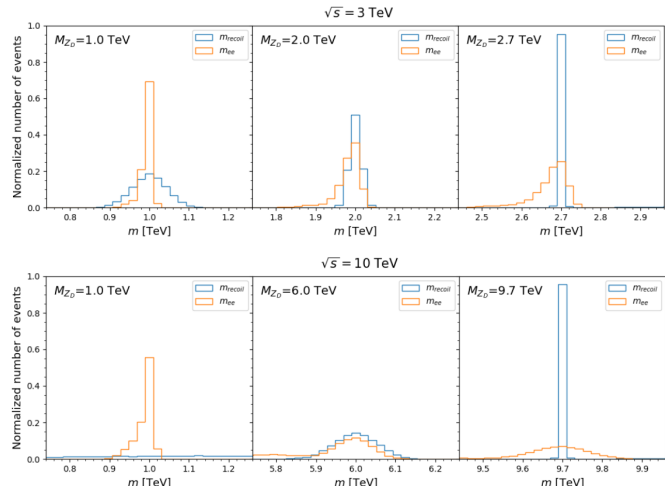
The recoil mass measures the mass of  $Z_D$  independent of its decay mode.

- At the detector, the photon recoil mass ( $m_{\text{recoil}}$ ) and  $e^+e^-$  invariant mass ( $m_{ee}$ ) distributions depend strongly on the energy resolutions of  $\gamma$ ,  $e^-$ ,  $e^+$ .
- Typically the energy resolution is expressed as:

$$\left(\frac{\Delta E}{E}\right)^2 = \left(\frac{a(\eta)}{\sqrt{E}}\right)^2 + \left(\frac{b(\eta)}{E}\right)^2 + c(\eta)^2$$

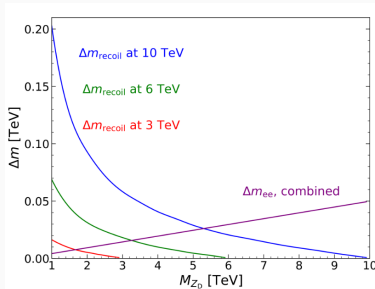
- $m_{Z_D} \rightarrow \sqrt{s}$ ,  $E_\gamma \rightarrow 0 \implies$  sharp photon  $m_{\text{recoil}}$  distribution.
- $m_{Z_D} \ll \sqrt{s}$ ,  $E_\gamma \gg 0 \implies$  broad photon  $m_{\text{recoil}}$  distribution.
- $m_{ee}$  distribution exhibits the opposite behavior.

Photon recoil mass  $m_{\text{recoil}}$  (blue) and the  $e^+e^-$  invariant mass  $m_{ee}$  (orange) for  $\mu^+\mu^- \rightarrow Z_D(\rightarrow e^+e^-)\gamma$  at  $\sqrt{s} = 3$  TeV and 10 TeV MuC.



Kingman Cheung, Jinheung Kim, Soojin Lee, Prasenjit Sanyal, Jeonghyeon Song,  
 Phys. Rev. D 112 (2025) 9, 095010

The  $m_{\text{recoil}}$  and  $m_{ee}$  distributions were then fitted with Gaussian distributions to obtain the widths  $\Delta m_{\text{recoil}}$  and  $\Delta m_{ee}$  as the standard deviations of the Gaussian fits.



Kingman Cheung, Jinheung Kim, Soojin Lee, **Prasenjit Sanyal, Jeonghyeon Song**,  
Phys.Rev.D 112 (2025) 9, 095010

Key characteristics:

1.  $\Delta m_{\text{recoil}}$  decreases with increasing  $m_{Z_D}$ .
2. For a fixed  $m_{Z_D}$ ,  $\Delta m_{\text{recoil}}$  increases with  $\sqrt{s}$ .
3.  $m_{ee}$  increases with  $m_{Z_D}$ .
4.  $\Delta m_{\text{recoil}}$  and  $m_{ee}$  intersects around  $m_{Z_D} \simeq \sqrt{s}/2$ .

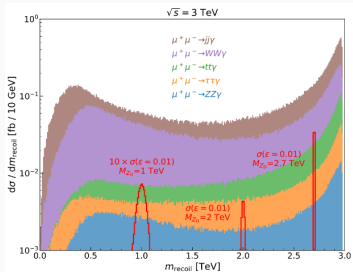
# Signal and background

- We consider scattering processes within  $|\eta| < 2.5$ ;  $p_T^\gamma > 20$  GeV;  $p_T^{j_1, e_1} > 100$  GeV and  $p_T^{j_2, e_2} > 20$  GeV for the leading and subleading jets or electrons.
- To categorize the two channels we require:

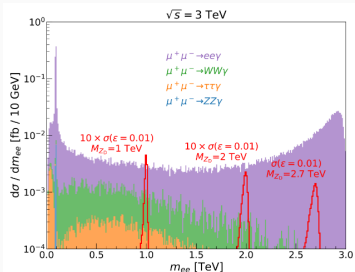
$$jjX \quad \begin{cases} N_j \geq 2 & N_\gamma \geq 1 \\ N_{e,\mu} = 0 & \text{lepton veto with } p_T > 20 \text{ GeV} \end{cases}$$

and

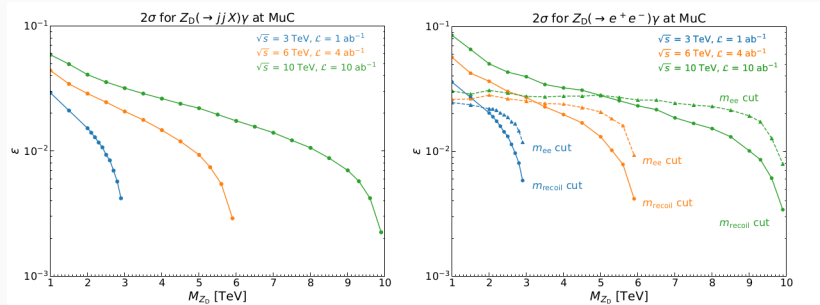
$$e^+ e^- \gamma \quad \begin{cases} N_e \geq 2 & N_\gamma \geq 1 \\ N_j = 0 & \text{jet veto with } p_T > 20 \text{ GeV} \end{cases}$$



- Two different mass window cuts:
  - $m_{\text{recoil}} = m_{Z_D} \pm 2\Delta m_{\text{recoil}}$
  - $m_{ee} = m_{Z_D} \pm 2\Delta m_{ee}$
- Dominant backgrounds:
  - $\mu^+ \mu^- \rightarrow jj\gamma$
  - $\mu^+ \mu^- \rightarrow e^+ e^- \gamma$



2 $\sigma$  contours for detecting  $Z_D$  through the processes:  $\mu^+\mu^- \rightarrow Z_D(\rightarrow jjX)\gamma$  (left) and  $\mu^+\mu^- \rightarrow Z_D(\rightarrow e^+e^-)\gamma$  (right).



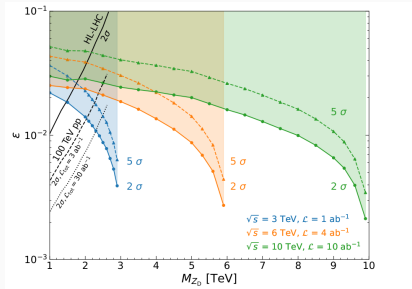
Phys.Rev.D 112 (2025) 9, 095010

- $jjX$  mode,  $m_{\text{recoil}}$  selection cut can be used only.
- $ee\gamma$  mode, both the  $m_{\text{recoil}}$  and  $m_{ee}$  selection cuts can be used.
- For the  $ee\gamma$  mode, the optimum choice is:  $m_{\text{recoil}}$  cut for  $m_{Z_D} > \sqrt{s}/2$  and  $m_{ee}$  cut for  $m_{Z_D} < \sqrt{s}/2$ .
- Statistical significance:

$$\mathcal{S} = \sqrt{2 \left[ (n_s + n_b) \ln \left( \frac{n_s + n_b}{n_b} \right) - n_s \right]}, \quad \mathcal{S}_{\text{tot}} = \sqrt{\mathcal{S}_{jjX}^2 + \mathcal{S}_{ee\gamma}^2}$$

# Results

2 $\sigma$  (solid lines) and 5 $\sigma$  (dashed lines) contours for detecting  $Z_D$ , combining the processes:  $\mu^+\mu^- \rightarrow Z_D(\rightarrow jjX)\gamma$  and  $\mu^+\mu^- \rightarrow Z_D(\rightarrow e^+e^-)\gamma$ .



Phys. Rev. D 112 (2025) 9, 095010

- The  $e\bar{e}\gamma$  mode outperforms at low  $m_{Z_D}$  and  $jjX$  mode outperforms at high  $m_{Z_D}$ . The improvement of combining both the channels is between 3% – 10%.
- 2 $\sigma$  contours of HL-LHC and FCC-hh shows that MuC clearly outperforms at higher  $m_{Z_D}$ .

## Conclusions

---

- Brief overview of dark  $Z_D$  boson. Current constraints and future sensitivities on the  $m_{Z_D} - \varepsilon$  space.
- Brief discussion on muon colliders as future collider experiment.
- Search for heavy  $Z_D$  at MuC via annihilation channel  $\mu^+ \mu^- \rightarrow Z_D \gamma$ .
- Optimised the photon recoil mass and the electron-positron invariant mass cuts to achieve the best sensitivity.

Background cross sections in units of fb			
Processes	$\sqrt{s} = 3$ TeV	$\sqrt{s} = 6$ TeV	$\sqrt{s} = 10$ TeV
$\mu^+ \mu^- \rightarrow jj\gamma$	$5.01 \times 10$	$1.40 \times 10$	5.44
$\mu^+ \mu^- \rightarrow e^+ e^- \gamma$	9.31	2.75	1.10
$\mu^+ \mu^- \rightarrow W^+ W^- \gamma$	$2.55 \times 10$	$1.01 \times 10$	4.86
$\mu^+ \mu^- \rightarrow \tau^+ \tau^- \gamma$	5.37	1.63	$6.67 \times 10^{-1}$
$\mu^+ \mu^- \rightarrow t\bar{t}\gamma$	3.24	1.07	$4.58 \times 10^{-1}$
$\mu^+ \mu^- \rightarrow ZZ\gamma$	2.25	$8.30 \times 10^{-1}$	$3.82 \times 10^{-1}$

Background cross sections

Cut-flow of cross sections (fb) for $\mu^+\mu^- \rightarrow Z_D(\rightarrow jjX)\gamma$ at a 3 TeV MuC with $\mathcal{L}_{\text{tot}} = 1 \text{ ab}^{-1}$						
$M_{Z_D} = 1 \text{ TeV} \ \& \ \varepsilon = 0.01$						
Cut	$Z_D(\rightarrow jj)\gamma$	$jj\gamma$	$W^+W^-\gamma$	$\tau^+\tau^-\gamma$	$t\bar{t}\gamma$	$\mathcal{S}_{1 \text{ ab}^{-1}}$
Basic	$7.69 \times 10^{-3}$	$1.42 \times 10$	$1.15 \times 10$	1.08	1.86	$4.47 \times 10^{-2}$
$ m_{j_1} - m_W  > 20 \text{ GeV}$	$6.34 \times 10^{-3}$	$1.20 \times 10$	3.75	1.08	1.51	$4.64 \times 10^{-2}$
$ m_{\text{recoil}} - M_{Z_D}  < 2\Delta m_{\text{recoil}}$	$3.47 \times 10^{-3}$	$9.37 \times 10^{-2}$	$8.47 \times 10^{-2}$	$1.01 \times 10^{-2}$	$1.29 \times 10^{-2}$	$2.40 \times 10^{-1}$
$M_{Z_D} = 2.7 \text{ TeV} \ \& \ \varepsilon = 0.01$						
$ m_{\text{recoil}} - M_{Z_D}  < 2\Delta m_{\text{recoil}}$	$3.12 \times 10^{-2}$	$3.32 \times 10^{-2}$	$6.22 \times 10^{-3}$	$4.20 \times 10^{-3}$	$7.72 \times 10^{-3}$	3.96

Table II: Cut-flow of cross sections in units of fb for the signal  $\mu^+\mu^- \rightarrow Z_D(\rightarrow jjX)\gamma$  with  $\varepsilon = 0.01$  and  $M_{Z_D} = 1 \text{ TeV}$  and  $2.7 \text{ TeV}$  at the 3 TeV MuC. The significance  $\mathcal{S}_{1 \text{ ab}^{-1}}$  is calculated assuming an integrated luminosity of  $1 \text{ ab}^{-1}$ . Note that  $\Delta m_{\text{recoil}}$  and  $\Delta m_{ee}$  values depend on  $M_{Z_D}$ .

Cut-flow of cross sections [fb] for $\mu^+\mu^- \rightarrow Z_D(\rightarrow jjX)\gamma$ at a 10 TeV MuC with $\mathcal{L}_{\text{tot}} = 10 \text{ ab}^{-1}$						
$M_{Z_D} = 1 \text{ TeV} \ \& \ \varepsilon = 0.01$						
Cut	$Z_D(\rightarrow jj)\gamma$	$jj\gamma$	$W^+W^-\gamma$	$\tau^+\tau^-\gamma$	$t\bar{t}\gamma$	$\mathcal{S}_{10 \text{ ab}^{-1}}$
Basic	$5.09 \times 10^{-4}$	1.21	1.86	$1.37 \times 10^{-1}$	$2.91 \times 10^{-1}$	$2.69 \times 10^{-2}$
$ m_{j_1} - m_W  > 20 \text{ GeV}$	$4.02 \times 10^{-4}$	$9.25 \times 10^{-1}$	$5.14 \times 10^{-1}$	$1.33 \times 10^{-1}$	$2.78 \times 10^{-1}$	$2.93 \times 10^{-2}$
$ m_{\text{recoil}} - M_{Z_D}  < 2\Delta m_{\text{recoil}}$	$2.28 \times 10^{-4}$	$4.55 \times 10^{-2}$	$9.00 \times 10^{-2}$	$4.49 \times 10^{-3}$	$9.23 \times 10^{-3}$	$5.85 \times 10^{-2}$
$M_{Z_D} = 9.7 \text{ TeV} \ \& \ \varepsilon = 0.01$						
$ m_{\text{recoil}} - M_{Z_D}  < 2\Delta m_{\text{recoil}}$	$1.18 \times 10^{-2}$	$3.18 \times 10^{-3}$	$9.43 \times 10^{-4}$	$3.95 \times 10^{-4}$	$1.20 \times 10^{-3}$	12.4

Table III: Cut-flow of the cross sections in units of fb for the signal  $\mu^+\mu^- \rightarrow Z_D(\rightarrow jjX)\gamma$  with  $\varepsilon = 0.01$  and  $M_{Z_D} = 1 \text{ TeV}, 9.7 \text{ TeV}$  at the 10 TeV MuC. The significance  $\mathcal{S}_{10 \text{ ab}^{-1}}$  is calculated considering an integrated luminosity of  $10 \text{ ab}^{-1}$ . Note that  $\Delta m_{\text{recoil}}$  and  $\Delta m_{ee}$  values depend on  $M_{Z_D}$ .

Final selection results for $\mu^+\mu^- \rightarrow Z_D(\rightarrow e^+e^-)\gamma$ at a 3 TeV MuC with $\mathcal{L}_{\text{tot}} = 1 \text{ ab}^{-1}$						
	$m_{\text{recoil}}$ cut		$m_{ee}$ cut		combined	
	$\sigma_{\text{sig}}$ [fb]	$\mathcal{S}_{1 \text{ ab}^{-1}}$	$\sigma_{\text{sig}}$ [fb]	$\mathcal{S}_{1 \text{ ab}^{-1}}$	$\sigma_{\text{sig}}$ [fb]	$\mathcal{S}_{1 \text{ ab}^{-1}}$
$M_{Z_D} = 1 \text{ TeV}$	$6.01 \times 10^{-4}$	$1.69 \times 10^{-1}$	$6.88 \times 10^{-4}$	$3.75 \times 10^{-1}$	$3.79 \times 10^{-4}$	$3.04 \times 10^{-1}$
$M_{Z_D} = 2.7 \text{ TeV}$	$5.91 \times 10^{-3}$	2.12	$5.71 \times 10^{-3}$	$7.37 \times 10^{-1}$	$3.23 \times 10^{-3}$	1.61

Table V: Signal cross sections and significances for  $\mu^+\mu^- \rightarrow Z_D(\rightarrow e^+e^-)\gamma$  at a 3 TeV MuC with  $\mathcal{L}_{\text{tot}} = 1 \text{ ab}^{-1}$ , shown for  $M_{Z_D} = 1 \text{ TeV}$  and  $M_{Z_D} = 2.7 \text{ TeV}$ . We fixed  $\varepsilon = 0.01$ . Results are presented after basic selection,  $E_{ee\gamma} > 0.9\sqrt{s}$  cut, and three final selection criteria: (1)  $m_{\text{recoil}}$  cut, (2)  $m_{ee}$  cut, and (3) combined cut applying both conditions.